NUCET NUCLEAR ENERGY AND TECHNOLOGY

Nuclear Energy and Technology 6(1): 49–54
DOI 10.3897/nucet.6.51781

Research Article

High-power electron accelerator for the production of neutrons and radioisotopes*

Elena A. Onishchyuk[1,2], Yury A. Kurachenko[3], Evgeny S. Matusevich[1]

1 *Obninsk Institute for Nuclear Power Engineering, National Research Nuclear University "MEPhI", 1 Studgorodok, Obninsk, Kaluga reg., 249040, Russia*

2 *Rosatom Technical Academy, 21 Kurchatov str., Obninsk, Kaluga reg., 249031, Russia*

3 *Russian Institute of Radiology and Agroecology, RIRAE, 109th km of Kiev hwy, Obninsk, Kaluga reg., 249032, Russia*

Corresponding author: Yury A. Kurachenko (ykurachenko@mail.ru)

Academic editor: Yury Kazansky ♦ **Received** 25 August 2019 ♦ **Accepted** 1 December 2019 ♦ **Published** 27 March 2020

Citation: Onishchyuk EA, Kurachenk YuA, Matusevich ES (2020) High-power electron accelerator for the production of neutrons and radioisotopes. Nuclear Energy and Technology 6(1): 49–54. https://doi.org/10.3897/nucet.6.51781

Abstract

The purpose of the work is to study the possible use of existing high-power electron accelerators for neutron therapy and the production of radioisotopes. Calculations were performed for both applications and the results were normalized to the characteristics of the existing MEVEX accelerator (average electron current 4 mA at a monoenergetic electron beam of 35 MeV). A unifying problem for the applications is the task of cooling the target: at a beam energy of about 140 kW, almost half of this energy is released directly in the target. For this reason, a liquid heavy metal was chosen as a target in order to combine the high quality of thermohydraulics with the maximum performance of both bremsstrahlung radiation and photoneutrons. The targets were optimized using precision codes for radiation transfer and thermal-hydraulic applications. Optimization was also carried out on the installation as a whole: (1) on the composition of the material and the configuration of the photoneutron extraction unit for neutron capture therapy (NCT) and (2) on the bremsstrahlung generation scheme for producing radioisotopes. The photoneutron unit provides an acceptable beam quality for NCT with a large neutron flux density at the output: ~ $2 \cdot 10^{10}$ $cm^{-2}s^{-1}$, which is an order of magnitude higher than the output values of existing and planned reactor beams. Such intensity at the beam output will make it possible in many cases to abandon fractionated irradiation. As for the production of radioisotopes, in the calculations for the (γ, n) reaction, 43 radionuclides in five groups were obtained. For example, using the $Mo^{100}(\gamma, n)^{99}Mo$ reaction, it is possible to obtain the ^{99}Mo precursor of the main diagnostic isotope ^{99m}Tc with a specific activity of ~ 6 Ci/g and a total target activity of 1.8 kCi after irradiation for 24 hours. The proposed schemes for generating and outputting photoneutrons and bremsstrahlung have a number of obvious advantages over traditional methods, including: (a) the use of electron accelerators for producing neutrons is much safer and cheaper than the use of reactor beams; (b) the accelerator with the target and the beam extraction unit with the necessary equipment and tooling can be easily placed in a clinical setting; and (c) the proposed liquid gallium target for NCT, which also serves as a coolant, is an "environmentally friendly" material: its activation is relatively small and drops quickly (after about four days) to the background level.

Keywords

Electron accelerator, photoneutrons, neutron capture therapy, beam modernization, high flux density, radioisotope production, (γ, n) reaction, ^{100}Mo production, unique beam characteristics, compact clinical installation

* Russian text published: Izvestiya vuzov. Yadernaya Energetika (ISSN 0204-3327), 2019, n. 4, pp. 142–152.

Introduction

A powerful photoneutron source for medical use was considered in (Kurachenko et al. 2012). In (Kurachenko 2014), the optimal configuration of the photoneutron beam extraction unit for neutron capture therapy (NCT) was obtained and, in (Kurachenko et al. 2016, 2017), the thermohydraulics of a combined flow target (W+Ga) and the possibility of using the beam for radiation therapy were studied. The fixed fragment of the target, i.e., a high-melting tungsten matrix, through which gallium flows, makes it possible to drastically increase the output of photoneutrons as compared to the target only from gallium. To normalize the calculation results, we used the data of the available MEVEX accelerator (MEVEX): 4 mA average current at an electron energy of 35 MeV.

Natural gallium is represented by two isotopes: ^{69}Ga (60.1%)+^{71}Ga (39.9%). It is a low-melting metal (t_{melt} = 29.8 °C) with a density of 5.904 g/cm^3 in the solid state and 6.095 g/cm^3 in the liquid state. Being melted, gallium for a long time remains in the liquid phase at room temperature. Moreover, gallium has a wide temperature range of the liquid phase (~ 2200 °C); therefore, the radiation energy release can be quite simply removed (Kurachenko et al. 2016).

The activation of natural gallium occurs due to photoreactions and reactions under the influence of intrinsic neutrons. The main processes: ^{69,71}Ga(γ, n)^{68,70}Ga, ^{69,71}Ga(n, 2n)^{68,70}Ga, ^{69,71}Ga(n, γ)^{70,72}Ga lead to short-lived products of reactions ^{68}Ga ($T_{1/2}$ = 68.3 min), ^{70}Ga ($T_{1/2}$ = 21.2 min) и ^{72}Ga ($T_{1/2}$ = 14.1 h). As calculations show, upon generation of neutron fields acceptable for NCT, and subject to the circulation of the target working fluid, the total gallium activity (for typical irradiation scenarios and the number of sessions) decreases to the level of the natural background in a time not exceeding four days (Fig. 1).

The results presented below were obtained in calculations of radiation transport (the MCNP5 code (LA-UR-03-1987 2003)) using the TENDL-2014/2017 nuclear data library based on the TALYS-1.9 nuclear reaction program (Koning et al. 2019). The target thermohydraulics was calculated using the STAR-CD code (Code Review).

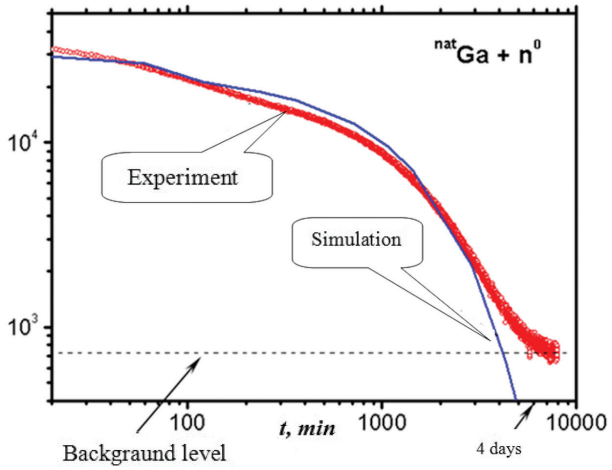

Figure 1. Activity decay of Gallium after typical irradiation scenario (rel. units).

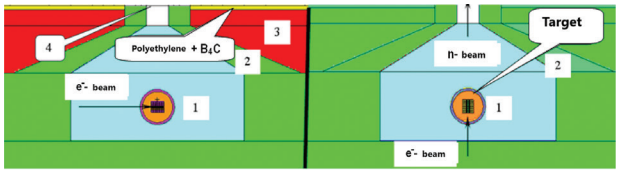

Figure 2. Axial sections of the axisymmetric beam extraction unit for NCT: "best" version from (Kurachenko et al. 2017) to the left and modernized version to the right (MCNP5 (LA-UR-03-1987 2003) input visualization). The fragments of the removal unit with a collimation system are presented: a channel filled with a spectrum shifter (1, lead fluoride PbF_2, also performs the function of a gamma filter); the channel is surrounded by the cone collimator (2, Pb, the main function is the slowing down and canalization of neutrons); zirconium hydride $ZrH_{1.8}$ (3) in the collimating system is a light shielding; the borated polyethylene and Cd plate 1 mm thick (4) at the outlet of the channel are a thermal neutron filter.

Photoneutron generation

NCT beam modernization

Beam modernization was aimed at increasing the neutron flux density at the output without impairing the beam characteristics essential for NCT and patient protection. For modernization, the beam extraction option with the maximum flux density at the output was chosen (Kurachenko et al. 2017). Figure 2 compares the cross sections of the optimal version of the beam extraction unit (Kurachenko et al. 2017) and the version proposed in this work.

The beam extraction unit is an axisymmetric assembly of cylindrical and conical layers; it performs protective and collimating functions (a conical layer of lead) as well as the functions of a spectrum shaper required for NCT.

The figure shows fragments of the extraction unit with a collimation system: a channel filled with a spectrum shaper (1 – lead difluoride PbF_2, which also performs the function of a gamma filter); the channel is surrounded by a collimator (2 – Pb, its main function is to slow down and channel neutrons). In the collimation system, zirconium hydride $ZrH_{1.8}$ (3) has the function of light protection; at the channel output, borated polyethylene and a 1 mm thick Cd plate (4) serve as a thermal neutron filter.

During the interaction of accelerated electrons with the massive W+Ga target, the main channel for energy loss is bremsstrahlung. At electron energies above 8–10 MeV, the bremsstrahlung gamma rays are absorbed by the Ga and W nuclei and produce neutrons in the (γ, n) reactions in the so called Giant Dipole Resonance (GDR) region with relatively large cross sections. Thus, the maximum (γ, n) cross sections on the main isotopes of natural W at an energy of ~ 15 MeV lie in the range 490–670 mb, for ^{69}Ga and ^{71}Ga, 102 mb at 17 MeV and 160 mb at 19 MeV, respectively.

Additional calculations made it possible to justifiably made changes to the configuration and material composi-

tion of the beam extraction unit in order to safely increase the main functional, i.e., the epithermal neutron flux density at the beam output.

These changes were as follows:

– the Cd plate at the channel output was removed, and the zirconium hydride layer was replaced with lead; the role of the removed materials in reducing the thermal neutron flux is negligible as epithermal neutrons entering the tissue generate near the input thermal backscattered neutrons, the intensity of which significantly exceeds the thermal neutron flux from the channel; and
– the combined flow target was placed coaxially with the neutron beam extraction axis and enclosed in a spherical tungsten housing filled with gallium. This measure made it possible to improve heat removal, increase neutron generation and reduce the output of "harmful" bremsstrahlung.

Beam quality for NCT

The beam quality for NCT is described by such characteristics as "in air" and "in phantom" (Kurachenko et al. 2017). The "in air" functionals characterize the radiation field at the beam output without an irradiated phantom and simplify the task of choosing the optimal configuration and composition of materials of the extraction unit (without time-consuming calculations of the "in phantom" functionals). It is assumed that, if the "in air" beam characteristics satisfy the specific criteria developed by the world community, then it should be expected that the "in phantom" functionals will also satisfy the NCT requirements.

To compare with the calculated beams from the target of the electron accelerator, the neutron beam characteristics of the existing and designed reactors are used:

– the FCB MIT beam, which is the "reference" for NCT (measurements (Riley et al. 2003), is currently decommissioned);
– the epithermal beam of the TAPIRO fast reactor (Agosteo et al. 2001) intended for use in NCT (the calculation was confirmed by measurements; the beam is decommissioned); and
– the beam of the specialized medical reactor MARS (calculation (Kurachenko 2008)).

The basic values of the "in air" characteristics for the compared beams are given in Tab. 1. For photoneutrons, data are presented on the "best" version (Kurachenko et al. 2017) and an updated version of the extraction unit (see Fig. 2, right). The actual criteria for NCT are given in Tab. 2. The above data indicate that, according to the criteria "in air" (or "for a free beam"), the proposed photoneutron beam is not inferior to, but even partially superior to the reactor beams for NCT. This conclusion is confirmed by Fig. 3, which shows the spectral characteristics of neutrons at the beam output.

Radioisotope generation

Model 1 (the simplest)

To produce radioisotopes according to Model 1 in the (n, γ) reaction, the conical moderator from lead difluoride was replaced with heavy water (see Fig. 2). The general configuration of the extraction unit does not change; samples are supposed to be irradiated at the channel output. It turned out that a significant thermalization of the beam at such a moderator depth (~ 0.5 m) could not be achieved: at Φ_{tot} =3.10×10^{10} cm^{-2}c^{-1} , the thermal neutron flux den-

Table 1. The flux density, spectral characteristics and average neutron energy at the yield of the reference, existing and projected reactor beams in comparison with the characteristics of photoneutron beams.

		Φ_{tot}, cm^{-2}c^{-1}, 10^9	Φ_{epi}/Φ_{tot}, %	Φ_{fast}/Φ_{tot}, %	Φ_{therm}/Φ_{tot}, %	E^{Φ}_{aver}, МэВ
NCT desired values		≥→ 1	~ 100	→ 0	→ 0	–
FCB MIT		4.2	No data available			
MARS		1.24	81.6	13.4	5.0	0.0337
TAPIRO		1.07	73.6	6.5	20.0	0.00857
Photo-neutrons	The "best" version (Kurachenko et al. 2017)	18.5	74.9	25.1	0.014	0.0345
	This paper	27.8	73.3	21.6	5.11	0.0325

Table 2. Actual NCT characteristics at the output of the reactor and photonuclear beams: epithermal neutron flux density, "poisoning" of the beam by gamma radiation and fast neutrons, direction.

		Φ_{epi}, cm^{-2}s^{-1}, 10^9	D_γ/Φ_{epi}, sGy·cm^2, 10^{-11}	D_{fast}/Φ_{epi}, сГр·см^2, 10^{-11}	J_{epi}/Φ_{epi} ("current-to-flux")
NCT desired values		≥ 1	< 2–5	< 2–5	≥ 0.7
FCB MIT		?	1.3	4.3.	0.8
MARS		1.01	5.38	11.8	0.8
TAPIRO		0.788	6.77	8.49	0.8
Photo-neutrons	The "best" version (Kurachenko et al. 2017)	13.9	0.0407	15.9	0.8
	this paper	20.4	0.0262	13.4	0.8

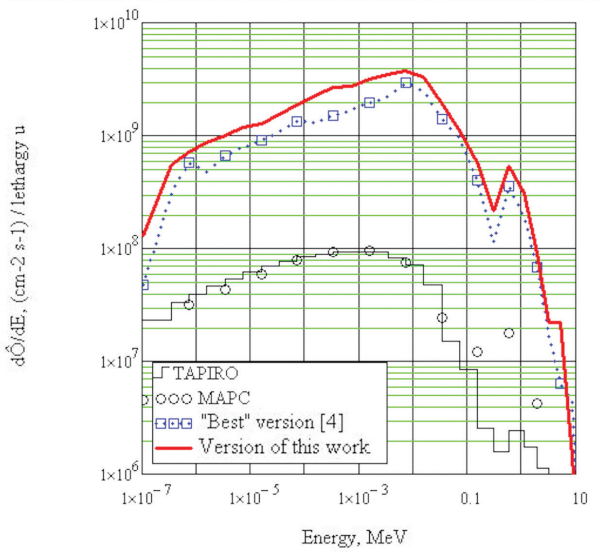

Figure 3. Neutron spectra at the beam outlet for NCT.

sity at the output was only Φ_{th} =1.24×10^{10} cm^{-2}c^{-1}. At the same time, in close proximity to the target, the thermal neutron flux density reaches ~ 2.5×10^{10}. When compared with the thermal neutron flux density in the reactor core, Model 1 turns out to be absolutely unpromising for the production of radioisotopes.

Model 2 (target with subcritical booster)

Figure 4 shows a model consisting of a cylindrical tank with heavy water. The target is located in the center of the tank and on the periphery is a subcritical assembly with k_{eff} ≤ 0.90 (assemblies with such subcriticality do not require a CPS during operation). The assembly consists of shortened BN-600 reactor fuel elements cooled by heavy water. The moderator is also D_2O. As a result of the calculation, a fairly aligned neutron field inside the tank was obtained. The maximum values of the neutron flux density Φ_{tot} = 6.19×10^{11} cm^{2}s^{-1} in close proximity to the target, the maximum thermal neutron flux density Φ_{th} = 3.09×10^{11} cm^{-2}s^{-1} is about 21 cm from the target. The neutron flux density increased by more than an order of magnitude as compared to the results obtained for the first mode. It is possible that under certain conditions the production of radioisotopes in the (n, γ) reaction according to Model 2 is practicable but it cannot compete with the reactor production.

Model 3 ((γ, n)-reactions)

This model turned out to be the most promising, since the bremsstrahlung output from the target is large enough. The considered cylindrical targets were optimized for the maximum bremsstrahlung output when an electron beam with a radius of 0.5 cm hit the cylinder end (Tab. 3, Fig. 5). The extrema in the optimization problems in this case are quite gentle; therefore, the step in the sizes of the targets is rough (0.25 cm). With the selected parameters of the electron beam, the bremsstrahlung output from the optimal targets is almost the same for all heavy materials. The average energy of bremsstrahlung lies in the GDP region near the energy of the maximum tungsten cross sections. For technological reasons, a lead-bismuth eutectic is preferred as a target; in this case, this alloy will also be a coolant.

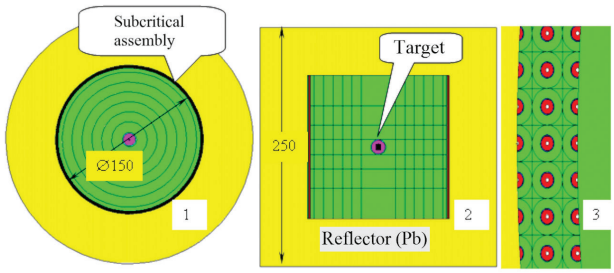

Figure 4. Radial (1) and axial (2) sections of model 2; (3) – fragment of the radial section with subcritical assembly (dimensions in cm).

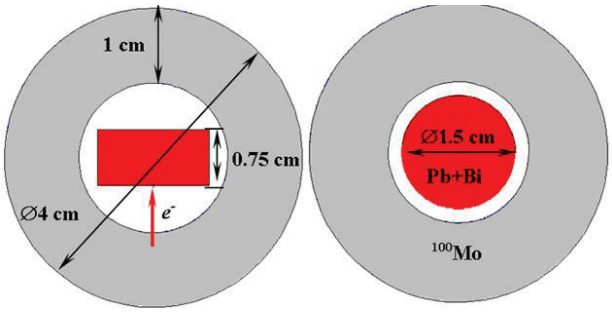

Figure 5. Sections of Spherical Computational Model 3 for the production of ^{99}Mo; the arrow shows the direction of the electron beam (visualization of the MCNP5 input file.

Let us estimate the production of ^{99}Mo by bremsstrahlung in the ^{100}Mo (γ, n)^{99}Mo reaction. A conventional irradiation scheme is shown in Fig. 5.

A cylindrical lead-bismuth target is enclosed in a spherical layer of the initial ^{100}Mo nuclide (Fig. 5). The equation for the production of ^{99}Mo can be written as follows:

$$d\rho^{99}/dt = \sigma\Phi_0\rho^{100} - \lambda\rho^{99}, \quad (1)$$

where ρ^{99}, ρ^{100} is the nuclear density (10^{24} cm^{-3}) of the produced and maternal isotope; $\sigma\Phi_0\rho^{100}$ is the rate of (γ, n) reactions, cm^{-3}s^{-1}; σ, Φ_0 are the group vectors of the cross section of the (γ, n) reaction (σ) and photon flux density (cm^{-2}s^{-1}) by the dimension of the tabular representation of the cross section (the energy group index is omitted); λ is the decay constant, s^{-1}.

Integration (1) in the irradiation time interval [0, t_{irr}], taking into account the initial condition $\rho^{99}(t = 0) = 0$, gives the density of the produced nuclei [cm^{-3}]:

$$\rho^{99} = \sigma\Phi_0\rho^{100}(1 - \exp(-\lambda t_{irr})) / \lambda; \quad (2)$$

specific activity [Bq×cm^{-3}] of the produced isotope A = λ × ρ^{99}; wherein

$$A = \sigma\Phi_0\rho^{100}(1 - \exp(-\lambda t_{irr})). \quad (3)$$

Table 3. Characteristics of the target for the radioisotope production according to Model 3.

Target material	Tl	Pb	Bi	^{238}U	Pb + Bi (45% +55%)
R, cm	1.0	0.75	0.75	0.50	0.75
H, cm	1.0	0.75	1.0	1.0	1.5
Density, g/cm^3	11.843	11.342	9.79	19.05	10.6
Melting point, °C	304	324	271	1133	124
Bremsstrahlung radiation, s^{-1}	1.29×10^{17}	1.32×10^{17}	1.34×10^{17}	1.25×10^{17}	1.33×10^{17}
Average energy, MeV	14.7	15.9	15.6	15.5	15.7

Table 4. Radioisotopes obtained in the calculation according to Model 3.

Isotope	$T_{1/2}$	Total activity, Ci	Specific activity, Ci/g
Positron emitters			
^{11}C (graphite)	20.39 min	140	2.22
^{13}N (boron nitride)	9.965 min	45.9	0.718
^{15}O (Be^{15}O)	122.24 s	104	1.17
^{18}F (Li^{18}F)	109.77 min	313	4.05
^{38}K	7.636 min	139	5.50
^{44}Sc	3.97 h	2250	25.7
^{45}Ti	184.8 min	3310	24.9
^{49}Cr	42.3 min	3550	16.9
^{62}Cu	9.673 min	3030	11.6
^{64}Cu	12.700 h	4240	[16.2]
^{63}Zn	38.47 min	2090	9.97
^{65}Zn	244.06 d	20.1	0.0962
^{68}Ga	67.71 min	6140	35.4
^{78}Br	6.46 min	1820	20.0
^{80}Br	17.68 min	2480	27.3
Diagnostic radioisotopes			
^{51}Cr	27.7025 d	208	0.984
^{54}Mn	312.12 d	9.15	0.0433
^{62}Cu	9.673 min	3030	11.6
^{64}Cu	12.700 h	4240	16.2
^{74}As	17.77 d	220	1.31
^{73}Se	7.15 h	3960	28.2
^{85}Sr	64.84 d	20.6	0.277
^{97}Ru	2.9days	2620	7.21
^{121}Te	19.16 d	123	0.672
^{139}Ce	137.64 d	30.9	0.156
^{140}Pr	3.39 min	3950	19.9
^{153}Gd	240.4 d	10.5	0.0453
^{157}Dy	8.14 h	6680	26.6
^{165}Er	10.36 h	5980	22.5
^{169}Yb	32.026 d	105	0.515
^{203}Hg	46.612 d	106	0.266
Radioisotopes for open source therapy			
^{88}Y	108.65 d	11.9	0.0911
^{97}Ru	2.9 d	2620	7.21
^{103}Pd	16.991 d	126	0.359
^{153}Sm	46.50 h	487	2.21
^{159}Gd	18.5 d	3330	14.4
^{169}Er	9.40 d	314	1.18
^{186}Re	3.7183 d	5040	8.18
^{192}Ir	73.827 d	4870	7.34
Radioisotopes for medical generators			
^{99}Mo	65.94 h	1780	5.96
^{113}Sn	115.09 d	54.4	0.0985
Long-lived positron sources for space			
^{150}Eu [1)]	$1.35 \cdot 10^4$ d	0.0385	0.000251
^{152}Eu [2)]	$4.94 \cdot 10^3$ d	0.528	0.00343

[1)] is the average positron energy of 0.22 MeV; [2)] is the average positron energy of 0.30 MeV

Let us compare the results with the data for the photonuclear reaction (γ, n) in (Bennett et al. 1999) during the production of ^{99}Mo at an electron accelerator with a power of 14 kW and an energy of 40 MeV (i.e., at an average current of 0.350 mA). For a highly enriched (96% ^{100}Mo) sample weighing 14.4 g at a 24-hour exposure, an activity of ~ 25

Ci or 1.74 Ci/g is performed (Bennett et al. 1999). Our data for the same exposure are 1.78 kCi and 5.96 Ci/g with a sample mass of 311 g, average current of 4 mA (MEVEX) and ^{100}Mo of 100% enrichment). Unfortunately, the specific irradiation geometry (Bennett et al. 1999) is not available. In (Kuplennikov et al. 2012), some information allows partial recovery of data (Kurachenko 2008).

The radionuclides generated according to Model 3 in the (γ, n) reaction (in the same geometry of Fig. 5 and under the same irradiation conditions) are presented in Tab. 4.

Conclusion

The compactness of modern powerful accelerators and good electron beam controllability make it possible to provide binary application of bremsstrahlung generated in the GPD region for the production of neutrons and radioisotopes. The proposed generation scheme has obvious advantages over reactor generation. First of all, it is ecological purity: the coolant activity decreases rapidly, there are no fission products in the installation, and the activation of the equipment is localized. In addition, the degree of radiation and nuclear safety is immeasurably higher as compared to reactor generation. Safety as well as the relatively small dimensions and weight of the installation allow it to be placed directly in a clinical setting. The epithermal neutron flux density (required for NCT) at the beam yield is at least an order of magnitude higher than the neutron flux density of the existing and planned reactor beams. Diversification in the alternative generation of medical radioisotopes in the same facility improves its economy and expands its capabilities. High generation efficiency of ^{99}Mo, the precursor of the main diagnostic radioisotope ^{99m}Tc (~ 80% of all procedures) is especially indicative.

References

- Agosteo S, Foglio Para A, Gambarini G, Casalini L, Burn KW, Tinti R, Rosi G, Festinesi A, Nava E (2001) Design of neutron beams for boron neutron capture therapy in a fast reactor. In: IAEA-TECDOC-1223: 116–125. https://www-pub.iaea.org/MTCD/Publications/PDF/te_1223_prn.pdf [accessed May 17, 2019]
- Bennett RG, Christian JD, Petti DA, Terry WK, Grover SB (1999) A System of ^{99m}Tc Production based on Distributed Electron Accelerators and Thermal Separation. Nuclear Technology 126: 102–121. https://doi.org/10.13182/NT99-A2961 [accessed May 17, 2019]
- Code Review. What is STAR-CD? http://www.procae.ru/articles/star-cd/76-about-star-cd.html [accessed May 17, 2019].
- Koning A, Hilaire S, Goriely S (2019) TALYS-1.9. A nuclear reaction program. ftp://ftp.nrg.eu/pub/www/talys/talys1.9.pdf 2017 [accessed May 17, 2019]
- Kuplennikov EL, Dovbnya AN, Tsymbal VA, Kandybey SS, Stoyanov AF (2012) Estimation of the ^{99}Mo and ^{99m}Tc production on the KhFTI ^{9}Be(d,n)-generator. VANT, 80(4): 155–159. https://vant.kipt.kharkov.ua/ARTICLE/VANT_2012_4/article_2012_4_155.pdf [accessed May 17, 2019] [in Russian]
- Kurachenko YuA (2008) Reactor beams for radiation therapy: quality criteria and computation technologies. Meditsinskaya Fizika [Medical Physics] 38(2): 20–28. [in Russian]
- Kurachenko YuA (2014) Photoneutrons for neutron capture therapy. Izvestiya vuzov. Yadernaya Energetika [News of Higher Educational Institutions. Nuclear Energy] 4: 41–51. https://doi.org/10.26583/npe.2014.4.05 [in Russian]
- Kurachenko YuA, Voznesensky NK, Goverdovsky AA, Rachkov VI (2012) New intensive neutron source for medical application. Meditsinskaya Fizika [Medical Physics] 38(2): 29–38. [in Russian]
- Kurachenko YuA, Zabaryansky YuG, Onishchuk HA (2017) Photoneutrons application for radiation therapy. Medicinskaya Radiologiya i Radiatsionnaya Bezopasnost [Medical Radiology and Radiation Safety] 62(3): 33–42. [in Russian]
- Kurachenko YuA, Zabaryansky YuG, Onishchuk YeA (2016) Optimization of the target for photoneutron production. Izvestia vuzov. Yadernaya Energetika [News of Higher Educational Institutions. Nuclear Energy] 3: 150–12. https://doi.org/10.26583/npe.2016.3.15 [in Russian]
- LA-UR-03-1987 (2003) Authors: X-5 Monte Carlo Team. MCNP – A General Monte Carlo N-Particle Transport Code, Ver. 5. Vol. I: Overview and Theory, 484 pp.
- MEVEX: The accelerator technology company. High Power Linacs for Isotope Production. http://www.mevex.com/Brochures/Brochure_High_Energy.pdf [accessed May 17, 2019]
- Riley KJ, Binns PJ, Harling OK (2003) Performance characteristics of the MIT fission converter based epithermal neutron beam. Physics in Medicine & Biology 48: 943–958. https://doi.org/10.1088/0031-9155/48/7/310